JOURNAL OF CATALYSIS 75, 354–374 (1982)

Adsorption Studies on Hydrodesulfurization Catalysts

I. Infrared and Volumetric Study of NO Adsorption on Alumina-Supported Co, Mo, and Co–Mo Catalysts in Their Calcined State

NAN-YU TOPSØE AND HENRIK TOPSØE

Haldor Topsøe Research Laboratories, DK-2800 Lyngby, Denmark

Received June 19, 1981; revised November 20, 1981

Infrared and volumetric studies were made of NO adsorbed on Co/Al_2O_3, Mo/Al_2O_3, and $Co–Mo/Al_2O_3$ oxide catalysts in order to elucidate the nature and amount of exposed Co and Mo ions. The effect of varying the cobalt loading, calcination temperature, and sample pretreatment conditions was studied. Bulk samples of Co_3O_4 and $CoAl_2O_4$ were also investigated. All Co-containing samples and catalysts give rise to two main infrared bands around 1780–1805 and 1850–1890 cm^{-1}. The details of the adsorption vary from system to system but in all cases NO seems to be predominantly adsorbed as a dinitrosyl (or dimeric) species. Low-loading Co/Al_2O_3 catalysts have a majority of the cobalt atoms located at the surface, in octahedral coordination. The remaining cobalt atoms are probably in tetrahedral coordination inside the alumina. As the cobalt loading increases the total number of cobalt atoms capable of adsorbing NO passes through a maximum, at which point formation of a separate Co_3O_4 phase is observed. This is accompanied by a decrease in the amount of cobalt atoms at the alumina surface. Upon increasing the calcination temperature some cobalt atoms move from octahedral sites at the surface to tetrahedral positions inside the alumina. Adsorption of NO on the $Co–Mo/Al_2O_3$ catalyst leads to an adsorption which differs from that on all the Co/Al_2O_3 catalysts. The results give evidence for formation of a Co–Mo interaction phase which is different from well-crystallized $CoMoO_4$ as well as the interaction phase observed for silica-supported catalysts. Increasing the calcination temperature causes a decrease in the number of cobalt atoms associated with the Co–Mo interaction phase. In contrast to previous studies, it is observed that $CoAl_2O_4$ adsorbs NO and that this is related to the spinel structure not being completely normal. Calcined Mo/Al_2O_3 catalysts only adsorb minor amounts of NO depending on the degree of reduction which has occurred during the sample pretreatment. The dominant adsorption seems to be in the form of dinitrosyls with bands around 1690–1710 and 1800–1810 cm^{-1}.

I. INTRODUCTION

Numerous studies by various techniques have been reported on $Co–Mo/Al_2O_3$ catalysts. One technique which has been used to characterize hydrodesulfurization (HDS) catalysts is infrared spectroscopy. Studies using this technique have mainly dealt with the calcined precursor state (*1–11*). However, recently (*12*) an investigation from this laboratory extended the ir work to *in situ* studies of sulfided catalysts. Some structural information concerning Co/Al_2O_3, Mo/Al_2O_3, and $Co–Mo/Al_2O_3$ catalysts was inferred through studies of the OH frequency region of these catalysts before and after sulfiding. The results confirmed the common belief that for calcined catalysts the molybdenum is present in a very high state of dispersion on the alumina surface. Furthermore, the results show that after typical sulfiding conditions the active components are also highly dispersed and are probably present as two-dimensional phases. Indications of interactions between cobalt and molybdenum were presented both for calcined and sulfided catalysts.

In order to gain more direct insight into the nature of the surface phases present in $Co–Mo/Al_2O_3$ catalysts, ir studies of the adsorption of selected probe molecules may be elucidative. Nitric oxide seems to be an ideal probe molecule for this purpose since

0021-9517/82/060354-21$02.00/0

it interacts strongly with transition metal ions but only weakly with typical support materials. Changes in NO bonding can also easily be detected by ir spectroscopy and such studies have already been widely carried out to characterize surface transition metal ions of supported metal and metal oxide catalysts (*13*). Recently, this type of investigation has been extended to calcined $Co-Mo/Al_2O_3$ catalysts (*9*, *10*), reduced Mo/Al_2O_3 catalysts (*14*), and thermally activated $Mo(CO)_6/Al_2O_3$ catalysts (*15*).

In the present paper, we report results of nitric oxide adsorption on Co/Al_2O_3, Mo/Al_2O_3, and $Co-Mo/Al_2O_3$ catalysts in their calcined state. The effects of changing parameters such as the metal loading and the calcination temperature are investigated. The ir studies are complemented by volumetric adsorption studies to obtain quantitative information. Studies on a few model compounds are also included in order to aid the interpretation of the results. A subsequent paper (*16*) will deal with NO adsorption on the catalysts in their sulfided and reduced states.

II. EXPERIMENTAL

The Co/Al_2O_3 (0.26% (wt), 2.0 or 6.5% Co), Mo/Al_2O_3 (8.0% Mo), and $Co-Mo/Al_2O_3$ (1.8% Co and 8.4% Mo) catalysts were prepared by depositing the active materials onto η-Al_2O_3 (surface area, 230 $m^2 g^{-1}$) via impregnation, or co-impregnation in the case of $Co-Mo/Al_2O_3$ (*17*), followed by drying and calcining at 773 K (923 K in some cases) in air for 2 h. The model compound $CoAl_2O_4$ was prepared by mixing citric acid with a solution containing the stoichiometric amounts of cobalt nitrate and aluminum nitrate. The mixture was then dried slowly at 313 K and calcined at 773 K (1073 K for some experiments) in air for 2 h. The bulk Co_3O_4 was prepared analogously leaving out the aluminum nitrate. Both these samples were checked by X-ray diffraction which showed them to be single phase and stoichiometric.

All the catalysts were ground and pressed (0.93 ton cm^{-2}) into self-supporting wafers 11 mg cm^{-2} in thickness and 2.86 cm in diameter. In the cases of the model compounds, wafers were prepared from physical mixtures of the samples and the Al_2O_3 carrier. The wafers were mounted in a stainless-steel holder and placed in an *in situ* quartz infrared cell with NaCl windows, which could be cooled by a water cooling jacket in thermal contact with each window. Heat shields inside the cell, which were removable by an external magnet during spectra recording, ensured that the temperature was constant during sample treatment and homogeneous across the sample wafer. The *in situ* cell allows treatment of the sample either under vacuum or in a flowing gas mixture at temperatures between 300 and 1000 K.

The pretreatment procedures of the samples before adsorption experiments are described in the following. The oxidic catalysts were pretreated by evacuating at 773 K (if not stated otherwise) for 16 h to 5×10^{-6} Torr and were subsequently cooled under vacuum to ambient temperature. In all cases, adsorption of NO was carried out at ambient temperature.

Infrared spectra were recorded with a Perkin–Elmer 180 grating spectrometer. The reference beam was appropriately attenuated to give reasonably good signal levels. A Nicolet model 535 signal averager was used such that the sloping background spectrum before NO adsorption could be subtracted from the spectrum of the sample after adsorption. Thus, in most cases only changes due to adsorption are reported. All quantitative information (including band intensity ratios) has been derived from absorbance spectra.

The volumetric chemisorption measurements were carried out at room temperature on a constant volume system, equipped with a Texas Instruments precision pressure gauge. Following a first isotherm, a second isotherm was obtained after evacuation for about 1 h. The amount of NO chemisorbed was obtained by either

taking the difference between the first and the second isotherm or by extrapolating the linear part of the first isotherm to zero pressure. Both methods gave quite similar results but only the values calculated from the latter procedure are given here.

The gases used in the experiments were purified as follows. Hydrogen was electrolytically generated and Pd-diffused in an Elhygen unit (Milton Roy Co.). Nitrogen was purified by passage through Cu turnings at 523 K and a molecular sieve trap (Linde 5A) kept at 195 K. Nitric oxide, 99% (AGA A/S), was further purified by the method described by Turnham (*18*). The gas was precooled to 195 K and passed slowly at this temperature through a trap of 12- to 28-mesh silica gel (Davison, grade 408, activated under vacuum for >2 h at 710 K and outgassed to $<3 \times 10^{-4}$ Torr at room temperature). The purified gas was then stored in a flask which had been evacuated to 10^{-6} Torr. Before use, the gas was frozen at 77 K and evacuated to remove nitrogen and then passed slowly through an *n*-pentane/liquid N_2 trap at 143 K to remove possible remaining traces of N_2O.

III. RESULTS

Blank NO adsorption experiments were carried out with the Al_2O_3 carrier pretreated in the same way as the catalysts. In no cases were absorption bands observed in the region 1600–2000 cm^{-1}.

(A) Mo/Al_2O_3

Adsorption of NO on the 8.0% Mo/Al_2O_3 catalyst, calcined at 773 K and evacuated at the same temperature for 16 h, gave weak bands at 1804 and 1693 cm^{-1} (Fig. 1a). The intensity of these bands was quite low and was found to depend on the evacuation temperature (Fig. 1). When the evacuation temperature was lowered from 773 to 723 K, the absorption bands became less intense (Fig. 1b) and no absorption bands were detected for samples evacuated at even lower temperatures (Fig. 1c). Although the bands observed after evacuation

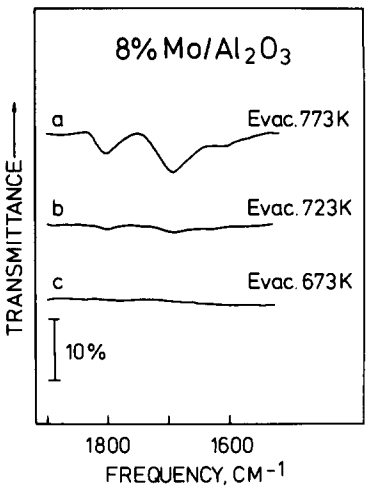

FIG. 1. Infrared spectra of NO adsorbed on an 8% Mo/Al_2O_3 catalyst after pretreatment by evacuation at: (a) 773 K; (b) 723 K; (c) 673 K.

at 723 K have low intensity, the intensity ratio, as well as the frequencies of the two bands, seems similar to that observed after evacuation at 773 K.

The spectra shown in Fig. 1 were obtained after adsorption and freezing out at 77 K the excess gaseous NO. In order to obtain information on the configuration of the adsorbed NO, spectra were recorded after various lengths of evacuation time at room temperature. For the sample pretreated at 773 K, this desorption treatment resulted in no change in either the total band intensities or the ratio of the two bands (Table 1). The ratio of the high-frequency to the low-frequency band was 0.63 in both cases. Also evacuation at 423 K did not result in significant changes in the spectra.

Studies were carried out on Mo/Al_2O_3 catalysts using different aluminas or preparation procedures. For example, a catalyst prepared by impregnating aluminum hydroxide gave almost no observable bands, whereas other catalysts gave bands at slightly higher frequencies than those reported above (Table 4).

The volumetric chemisorption of NO on the catalyst evacuated at 773 K (Table 2) gave only a very small uptake correspond-

TABLE 1

Infrared Parameters of NO Adsorption

Type	Sample	$\frac{I_A}{I_B}$[a]	$\frac{I'_A}{I'_B}$[b]	R[c]	$\frac{I'_A}{I_A}$	$\frac{I'_B}{I_B}$
I	$CoAl_2O_4$ calcined at 823 K	0.43	0.39	0.89	0.64	0.72
	$CoAl_2O_4$ calcined at 1073 K	0.47	0.40	0.86	0.61	0.71
II	0.26% Co/Al_2O_3	0.31	0.23	0.75	0.59	0.78
	2.0% Co/Al_2O_3 calcined at 773 K	0.39	0.31	0.81	0.65	0.80
	2.0% Co/Al_2O_3 calcined at 923 K	0.27	0.22	0.82	0.71	0.87
III	6.5% Co/Al_2O_3	0.70	0.43	0.62	0.39	0.64
	Co_3O_4	~3.06	1.23	0.40	0.24	~0.61
	10% Co 8% Mo/Al_2O_3	1.00	0.69	0.69	0.45	0.65
IV	2% Co 8% Mo/Al_2O_3 calcined at 773 K	0.46	0.46	0.99	0.96	0.97
	2% Co 8% Mo/Al_2O_3 calcined at 923 K	0.46	0.46	0.99	0.94	0.95
V	8% Mo/Al_2O_3	0.63	0.63	1.00	1.00	1.00

[a] I_A, I_B are intensities of absorption bands A (high-frequency) and B (low-frequency) after freezing out the excess gaseous NO at 77 K.

[b] I'_A, I'_B are intensities of absorption bands A and B after subsequent evacuation at room temperature.

[c] $R = (I'_A/I'_B)/(I_A/I_B)$.

TABLE 2

NO Chemisorption on Calcined Mo, Co, and Co–Mo/Al_2O_3 Catalysts

Catalyst	Catalyst pretreatment (calc. temp., K)	NO uptake (μmol/g)	NO uptake (mol NO/mol Co_{total} (or Mo_{total}))
		Co/Al_2O_3	
0.26% Co/Al_2O_3	773	44.6	1.02
0.26% Co/Al_2O_3	773	46.2	1.05
2% Co/Al_2O_3	773	167.9	0.49
2% Co/Al_2O_3	923	88.4	0.26
6.5% Co/Al_2O_3	773	86.1	0.078
		Co–Mo/Al_2O_3	
1.83% Co 8.4% Mo/Al_2O_3	773	82.6	0.27[a]
1.83% Co 8.4% Mo/Al_2O_3	773	73.0	0.24[a]
1.83% Co 8.4% Mo/Al_2O_3	923	39.4	0.13[a]
		Mo/Al_2O_3	
8% Mo/Al_2O_3	773	3.7	0.004

[a] Value based on total content of Co and not corrected for the small uptake on Mo.

ing to less than 1% of the Mo atoms adsorbing NO.

(B) Cobalt Model Compounds and Co/Al_2O_3 Catalysts

The cobalt-containing samples all show absorption bands in two frequency regions. The highest-frequency bands (denoted A) lie between 1850 and 1900 cm^{-1} whereas the low-frequency bands (denoted B) fall in the region of 1780–1800 cm^{-1}.

$CoAl_2O_4$

The present ir and volumetric results show that some adsorption of NO on $CoAl_2O_4$ does occur in contrast to previous findings by Yao and Shelef (*19*). The spectrum of NO adsorbed on $CoAl_2O_4$ calcined at 923 K (Fig. 2a) shows two bands. The A and B bands appear around 1875 and 1790 cm^{-1}, respectively. The spectrum in Fig. 2a was recorded after the sample had been exposed to NO for about 1 h and the gaseous NO and loosely bound NO had been removed by evacuation at room temperature. During the initial exposure to NO the bands did not vary appreciably with time but some changes occurred upon evacuation.

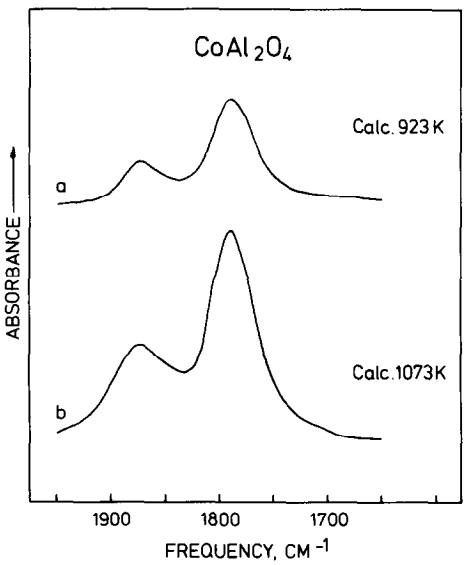

FIG. 2. Infrared spectra of NO adsorbed on $CoAl_2O_4$ calcined at: (a) 923 K; (b) 1073 K.

The spectra before evacuation (but after gaseous NO had been frozen out) and after evacuation have been characterized in Table 1 by a number of parameters. This table gives the ratio of the intensity of the A band to that of the B band, both for the spectra before and after evacuation (I_A/I_B and I'_A/I'_B, respectively). The changes occurring in the I_A/I_B ratio as a result of the evacuation are characterized by the parameter R defined as I'_A/I'_B divided by I_A/I_B. Table 1 also gives the change in the absorbances of the A and the B bands before and after evacuation (I'_A/I_A and I'_B/I_B).

It is seen that I_A/I_B is slightly smaller after evacuation than before ($R < 1$). This indicates that the A and B bands do not exclusively arise from one type of NO adsorption. The adsorption of NO on $CoAl_2O_4$ is not very strong since about 30% of the NO could easily be removed by room-temperature evacuation. After raising the evacuation temperature to 373 K absorption bands could still be observed, but further increase to 423 K resulted in complete removal of the bands. The I_A/I_B ratio during this desorption process was observed to remain constant indicating that the two bands in these spectra originate from the same adsorbed species. The higher I_A/I_B ratio before evacuation suggests that in these spectra another type of adsorbed NO, which is weakly bound, is also present and gives rise to NO stretching frequencies in the A band region.

NO adsorption was also studied on the $CoAl_2O_4$ sample after heating to 1073 K for 2 h (Fig. 2b).

It is seen from Fig. 2b that the total absorbance of the bands has increased but the frequencies of the A and B bands remain similar to those in Fig. 2a. Also, all the parameters in Table 1 are quite similar for the two samples. (In the following, this type of adsorption is referred to as Type I.) This shows that the high-temperature heat treatment has created more of the same type of

adsorption sites as those found in the sample treated at the lower temperature. The fraction of Co surface atoms adsorbing NO is actually larger in the high-temperature than in the low-temperature $CoAl_2O_4$ sample, since the specific surface area was found to be lower in the former sample.

To examine the apparent discrepancy between the present results and those previously reported (*19*), NO adsorption on $CoAl_2O_4$ was also measured volumetrically (Table 3). A rather great amount of adsorbed NO corresponding to a significant surface coverage is observed. Moreover, volumetric results confirm the trend observed in the ir data that the amount of adsorbed NO increased with an increase in pretreatment temperature.

Co_3O_4

In contrast to $CoAl_2O_4$, Co_3O_4 shows NO absorption spectra which change greatly upon evacuation after NO adsorption. Before evacuation (Figs. 3a and b) the spectrum appears mainly as a broad band consisting of contributions around 1780, 1850, and 1865 cm^{-1}. This band does not seem to vary with time of exposure to NO. However, upon evacuation (Fig. 3c) the contribution at 1850 cm^{-1} disappears. Readmission of NO to the evacuated sample produced essentially the same spectrum as before evacuation. Since the 1850-cm^{-1} band lies in the A band region, the ratio I_A/I_B is very high and the resulting R value is much less than one (Table 1). The type of adsorption giving the typical Co_3O_4 parameters is designated as Type III.

TABLE 3

NO Chemisorption on $CoAl_2O_4$ and Co_3O_4

Compound	NO uptake (μmol/g)	Surface area (BET) (m^2/g)	NO uptake (molecules/10^{-15} cm^2)
$CoAl_2O_4$[a]	119.4	52.9	0.14
Co_3O_4	52.8	6.28	0.51

[a] Calcined at 1073 K.

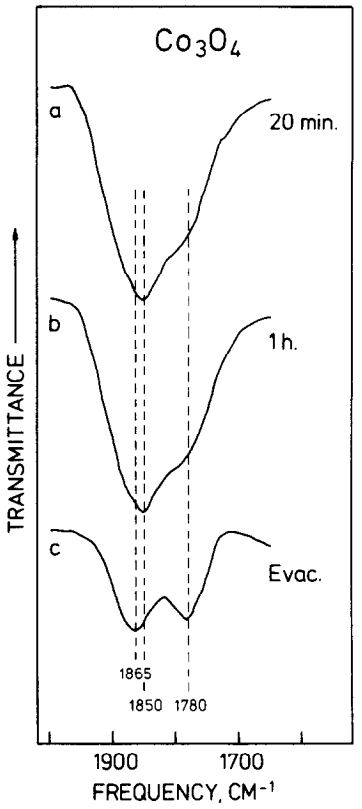

FIG. 3. Infrared spectra of Co_3O_4 recorded after adsorbing NO for: (a) 20 min; (b) 1 h; both with the excess NO frozen out at 77 K; (c) after subsequent evacuation of the sample at room temperature.

Before exposure to NO, the calcined Co_3O_4 sample was evacuated at 773 K for 16 h. X-Ray diffraction of this sample before evacuation showed stoichiometric Co_3O_4. However, after the evacuation pretreatment the diffraction pattern was largely that of CoO.

Volumetric adsorption of NO was studied for the Co_3O_4 sample (Table 3) and the amount of NO adsorbed (per BET surface area) is in rather good agreement with the value determined by Yao and Shelef (*19*).

Co/Al_2O_3 Catalysts

The Co/Al_2O_3 catalysts show two absorption bands (bands A and B) in the same frequency regions as those of $CoAl_2O_4$ and Co_3O_4, but the detailed nature of the NO adsorption of Co/Al_2O_3 catalysts depends

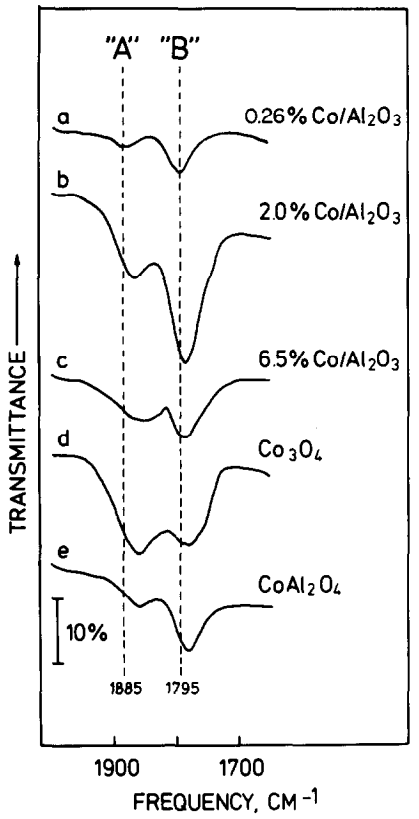

FIG. 4. Infrared spectra of NO adsorbed on: (a) 0.26% Co/Al_2O_3; (b) 2.0% Co/Al_2O_3; (c) 6.5% Co/Al_2O_3; (d) Co_3O_4; (e) $CoAl_2O_4$.

strongly on parameters such as the cobalt loading and the calcination temperature (Figs. 4–7).

Figures 4a–c show the changes which occur when the cobalt loading is varied for catalysts calcined at 773 K. The NO absorption spectra on the bulk Co_3O_4 and $CoAl_2O_4$ samples (Figs. 4d and e) are included for comparison. The 0.26% Co/Al_2O_3 sample calcined at 773 K shows upon NO adsorption an A band around 1885 cm^{-1} and a B band around 1795 cm^{-1}. These bands are shifted downwards in frequency with increasing Co loading, as seen for the 2.0% Co/Al_2O_3 (Fig. 4b) and the 6.5% Co/Al_2O_3 catalysts (Fig. 4c). The relative intensity of the two bands, I_A/I_B, increases with higher Co concentration (Fig. 5a). As indicated in Table 1 the adsorption of NO on the 0.26 and 2% Co catalysts (referred to as Type II) has many similarities with that of $CoAl_2O_4$ (Type I) but differs largely from that of Co_3O_4 (Type III). In contrast to the two lower-loading catalysts, the 6.5% Co/Al_2O_3 catalyst shows an adsorption behavior resembling that of Co_3O_4 (Table 1). For example, the spectrum of the 6.5% Co/Al_2O_3 catalyst (Fig. 4c) shows a broad A band with a large contribution at 1850 cm^{-1}. As for Co_3O_4 this contribution corresponds to weakly held NO, and was removed by evacuation at room temperature. The bands remaining after evacuation have frequencies similar to those for the Co_3O_4 sample.

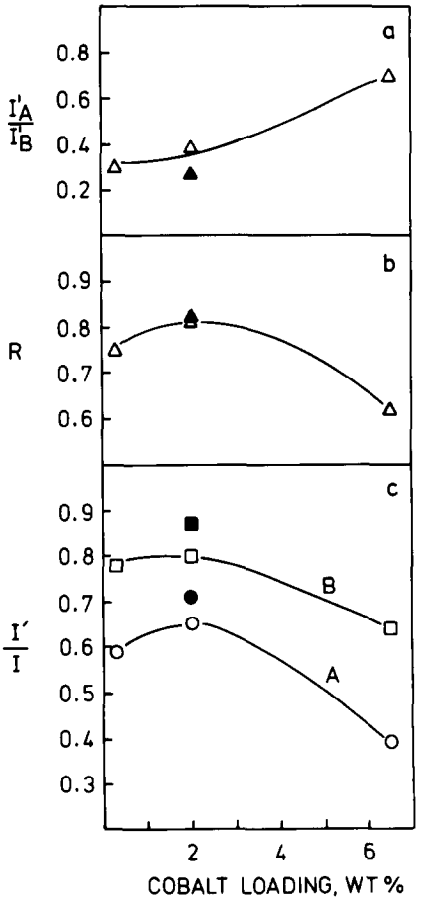

FIG. 5. Infrared intensity parameters of the NO absorption spectra of the Co/Al_2O_3 catalysts: (a) I'_A/I'_B; (b) R; (c) I'/I as a function of cobalt loading. The solid symbols represent the 2% Co/Al_2O_3 calcined at 923 K, whereas the open symbols represent catalysts calcined at 773 K.

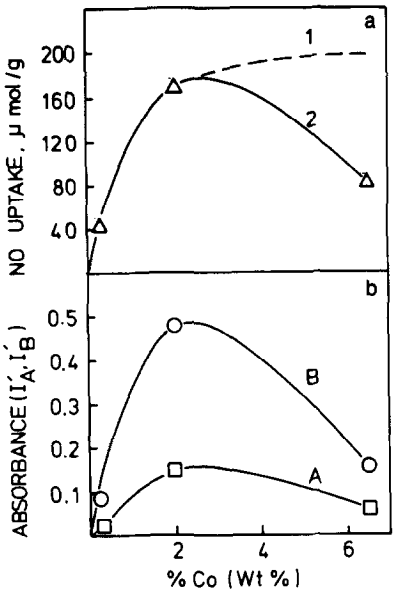

FIG. 6. Loading dependence of (a) NO uptake and (b) absorbances of NO absorption bands A and B for Co/Al_2O_3 catalysts calcined at 773 K. 1 and 2 refer to the variations expected from the two schemes pictured in Fig. 11.

The presence of Co_3O_4 in the 6.5% Co/Al_2O_3 catalyst was confirmed by Mössbauer (*20*) and X-ray diffraction measurements.

The spectra of the two low-loading Co/Al_2O_3 catalysts as a function of exposure time to NO show virtually no time dependence. Subsequent to NO adsorption, evacuation was carried out at increasing temperatures. The effects of room-temperature evacuation after NO adsorption are given in Table 1. For all the Co/Al_2O_3 catalysts, R is found to be less than one. This shows that the A band before evacuation contains contributions from a weakly adsorbed form of NO. Evacuation at higher temperatures resulted in a significant decrease in the absolute intensity of both bands A and B whereas the ratio of the two bands remained essentially unchanged from the value observed after pumping at room temperature. For example, for the 2% Co/Al_2O_3 catalyst it was found that raising the evacuation temperature from room temperature to 390 K resulted in a decrease in the total intensity by a factor of about 8, whereas by the same pretreatment the I_A/I_B ratio changed only insignificantly (from 0.28 to 0.29). Thus, it can be concluded that the A and B bands remaining after evacuation at room temperature are related to the same adsorption complex.

Figures 5 and 6 show the loading dependence of the I'_A/I'_B ratio (Fig. 5a), R (Fig. 5b), the I'_A/I_A and I'_B/I_B ratios (Fig. 5c), the NO uptake (Fig. 6a), and the total absorbance of the A and B bands after evacuation (Fig. 6b). When the loading is increased from 0.26 to 2.0% Co the absorbance (Fig. 6b) increases drastically, whereas the other spectral parameters (Figs. 5a–c) vary only slightly. Consequently, the main changes occurring when the cobalt loading is in-

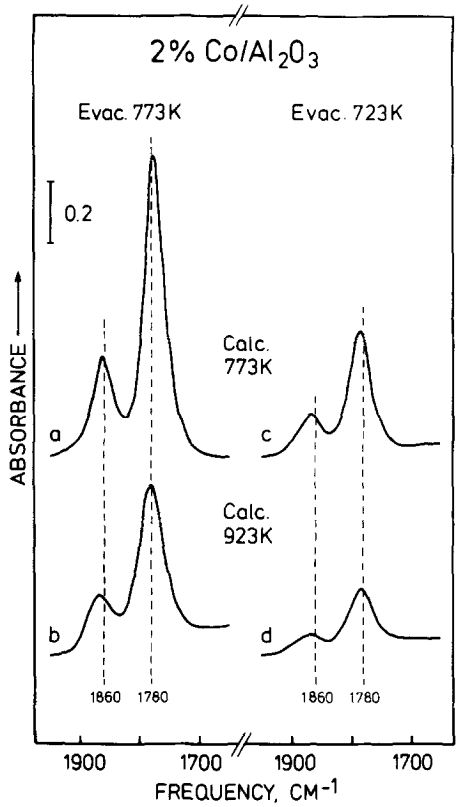

FIG. 7. Infrared spectra of NO adsorbed on 2% Co/Al_2O_3 catalyst calcined and evacuated, respectively, at: (a) 773 K and 773K; (b) 923 K and 773 K; (c) 773 K and 723 K; (d) 923 K and 723 K.

creased in this region involve formation of more of the same Co species. The results of independent volumetric chemisorption experiments provide additional information. It was observed that after pretreatment identical to that used in the ir experiments, the 0.26% Co/Al_2O_3 catalyst strongly chemisorbed 45 μmol NO/g catalyst. This corresponds to about 1.05 mol NO/mol Co in the catalyst. Thus, this result shows that for the low-loading catalyst the fraction of Co atoms at the surface must be very large. However, a further increase of the loading from about 2.0 to 6.5% Co results in an actual decrease in the total absorbance. This suggests the formation of a bulk Co phase which, as mentioned above, can be assigned to Co_3O_4.

It is seen in Fig. 6 that the loading dependence of chemisorbed NO is rather similar to the variation in the ir absorbances. The volumetric results show directly as mentioned above that a large fraction of Co is present at the surface of the low-loading catalyst containing 0.26% Co. The fraction of cobalt atoms adsorbing NO is still quite large for the 2.0% Co/Al_2O_3 catalyst but much smaller for the 6.5% Co/Al_2O_3 catalyst (Table 2).

The Co species at the surface of the alumina in the low-loading Co/Al_2O_3 catalysts resemble those present in $CoAl_2O_4$. There are, however, some distinct differences (Fig. 4 and Table 1). For the catalysts, the A and B bands appear at higher frequencies and the I_A/I_B and I'_A/I'_B ratios are smaller whereas both the R values and the I'_A/I_A and the I'_B/I_B ratios are greater.

The effect of increasing the calcination temperature to 923 K is shown in Fig. 7 for the 2% Co/Al_2O_3 catalyst, and some of the spectral parameters are included in Table 1 and Fig. 5. The main effect of such an increase is a decrease in the intensity of the absorption bands by a factor of about 2. Moreover, a slight shift in the band position toward higher frequencies is observed. This finding, as well as some of the other spectral parameter changes (Table 1), may suggest a type of adsorption that closely resembles that of the 0.26% Co/Al_2O_3 catalyst calcined at the lower temperature.

Increase in the evacuation temperature used in the pretreatment of the samples before NO adsorption was studied for the 2% Co/Al_2O_3 catalyst. Such a change is seen (Fig. 7) to result in an increased NO adsorption, but the effect is much less pronounced than that for the Mo/Al_2O_3 catalyst (Fig. 1). The higher evacuation temperature leads to a slight increase in the I_A/I_B ratio and a small frequency shift downwards.

(C) $Co-Mo/Al_2O_3$ Catalysts

The 1.8% Co 8.4% Mo/Al_2O_3 catalyst, calcined and evacuated at 773 K, showed after adsorption of NO (Fig. 8a) three absorption bands at 1880, 1796, and 1695 cm^{-1}. For comparison, the spectra of the 2% Co/Al_2O_3 (Fig. 8b) and the 8% Mo/Al_2O_3 (Fig. 8c) catalysts are also shown. These two individual component catalysts have about the same metal loading as that of the combined catalyst. Figure 8d shows an addition of the spectra of the 2% Co/Al_2O_3 and 8% Mo/Al_2O_3 catalysts. By comparing Figs. 8a and d it is obvious that there are many differences between the spectrum of the Co–Mo catalyst and the addition spectrum of the individual Co and to adsorption on cobalt. The 1796-cm^{-1} band contains contributions from adsorption both on cobalt and molybdenum but is dominated by the contribution of the former since the contribution of molybdenum as shown by the 1695-cm^{-1} band is rather weak. Qualitatively, these assignments agree with those of Peri (*9*) but differ from those of Hardee (*10*).

It is noteworthy that several results indicate that the cobalt atoms adsorbing NO in the $Co-Mo/Al_2O_3$ catalyst are different from those in the Co/Al_2O_3 sample. One striking difference is that for the catalyst also containing Mo, the frequencies of the Co bands are significantly higher than those

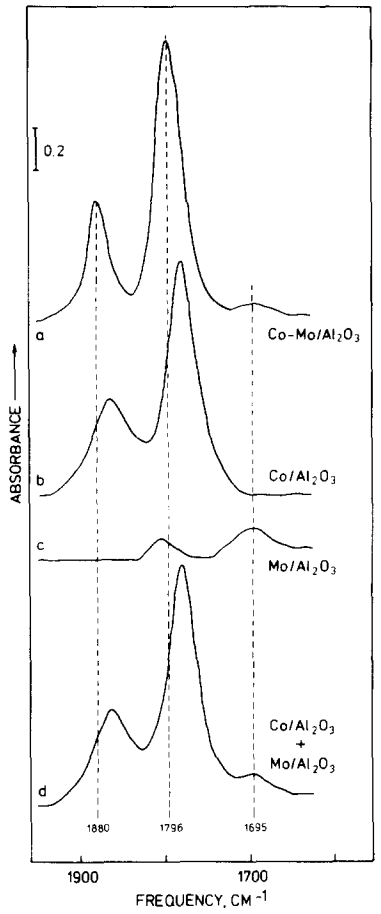

FIG. 8. Infrared spectra of NO adsorbed on: (a) Co–Mo/Al_2O_3; (b) Co/Al_2O_3; (c) Mo/Al_2O_3. Spectrum (d) is the theoretical sum spectrum obtained by adding (b) and (c).

for the catalyst that contains Co alone. The bands are also much narrower in the case of the combined catalysts. Moreover, the band intensities and the changes occurring after the evacuation are different in the two cases (Table 1). For the $Co–Mo/Al_2O_3$ catalyst the relative band intensity ratio I_A/I_B is around 0.46 and does not change after evacuation. This is also in contrast to the Co/Al_2O_3 catalyst which showed a lower intensity ratio which decreased upon evacuation. Furthermore, the absolute intensities of the A and B bands hardly decrease upon evacuation. The above characteristics of the adsorption of NO on the Co–Mo/Al_2O_3 catalyst are not only different from those of the adsorption of NO on the 2% Co/Al_2O_3 catalyst but also differ from those of the adsorption of NO on the higher- (6.5% Co) and the lower- (0.26% Co) loading Co/Al_2O_3 catalysts as well as on $CoAl_2O_4$ and Co_3O_4 (Table 1). To stress this distinction, the adsorption on the Co–Mo/Al_2O_3 catalyst is called Type IV in Table 1. The observation that the total integral intensities of the cobalt absorption bands are almost the same for the 1.8% Co 8.4% Mo/Al_2O_3 and the 2% Co/Al_2O_3 catalysts while the total NO uptakes (Table 2) on the two catalysts are quite different also suggests that the nature of the NO adsorption complex on the two systems is different.

Regarding the adsorption on the Mo atoms in the $Co–Mo/Al_2O_3$ catalyst definite conclusions are more difficult to reach since only the rather weak 1695-cm^{-1} band is resolved. Nevertheless, the frequency of this band is very similar to that observed in the Mo/Al_2O_3 catalyst (Fig. 8c) but a comparison of spectra a and c in Fig. 8 shows that the total intensity of the molybdenum band at 1695 cm^{-1} is slightly smaller for the Co–Mo/Al_2O_3 catalyst than for the catalyst containing only Mo.

Increase in the calcination temperature of the $Co–Mo/Al_2O_3$ catalyst from 773 to 923 K results (Fig. 9) in a noticeable intensity decrease of the two high-frequency bands associated with the Co atoms, as well as of the 1695-cm^{-1} band associated with Mo. At the same time, the bands shift upwards from 1880, 1796, and 1695 cm^{-1} to 1884, 1802, and around 1702 cm^{-1}, respectively. The relative intensity ratios (Table 1) are, however, the same as after calcination at 773 K. Thus, the main effect of increasing the calcination temperature is to decrease the number of cobalt sites at the surface but the remaining sites are quite similar to those in the catalyst calcined at the lower temperature.

The effect of increasing the Co loading was also investigated for the $Co–Mo/Al_2O_3$ catalyst. Figure 10 shows the spectra of a catalyst (calcined at 773 K) with an in-

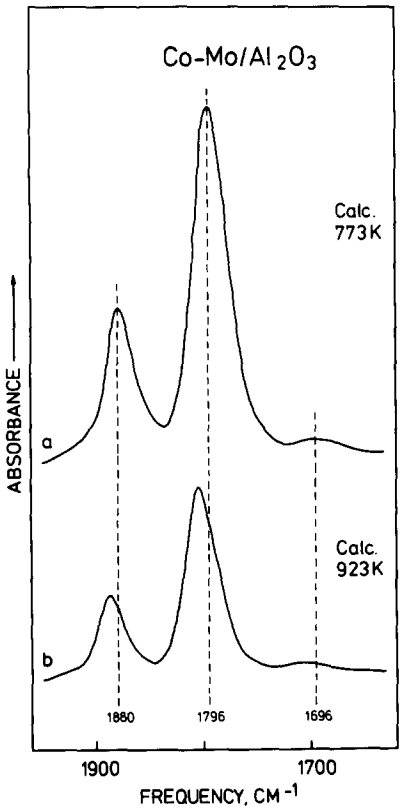

FIG. 9. Infrared spectra of NO adsorbed on Co–Mo/Al_2O_3 catalyst calcined at: (a) 773 K; (b) 923 K.

creased Co loading of 10.4%. The type of absorption observed is quite different from that of the low-loading Co–Mo/Al_2O_3 catalyst (Table 1) in that the I_A/I_B ratio is much higher and is sensitive to length of adsorption and evacuation ($R < 1$). The total band intensity also decreases significantly upon evacuation at room temperature. In fact, the adsorption behavior resembles in many respects the Type III adsorption behavior observed for the high-loading Co/Al_2O_3 catalyst and Co_3O_4. The presence of Co_3O_4 in this and other similar catalysts has indeed been revealed by Mössbauer spectroscopy (*20, 21*).

IV. DISCUSSION

Adsorption of NO on Co/Al_2O_3, Mo/Al_2O_3, and Co–Mo/Al_2O_3 catalysts gives rise to absorption bands in the region 1600 to 2000 cm^{-1}, whereas the Al_2O_3 carrier does not show bands in this region. It is seen that the frequencies and the intensities of the NO absorption bands depend, among other parameters, on the metal loading, the calcination temperature, and on whether Co or Mo or both elements are present. This reflects that changes occur both in the nature and in the abundance of the surface phases and indicates that NO adsorption is well suited as a probe of the surface chemistry of these catalysts.

NO is well known as a ligand in coordina-

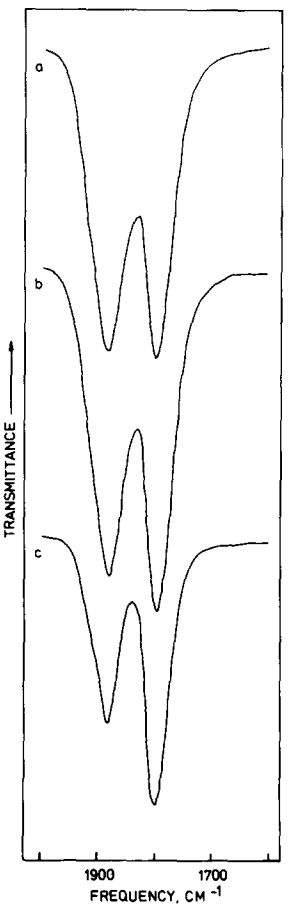

FIG. 10. Infrared spectra of NO adsorbed on Co–Mo/Al_2O_3 catalyst containing 10.4% Co and 7.6% Mo. Spectra (a) and (b) are obtained after 15 min and 2 h adsorption with NO, respectively. Spectrum (c) is obtained after subsequent evacuation at room temperature.

tion complexes of transition metals and, as with metal carbonyls, the accepted bonding picture is that of donation of electron density from nitrogen to the metal (σ bond) and back-bonding by the metal d electrons into the NO π^* orbital (*13, 22–24*). The greater the back-bonding into the antibonding π^* orbital, the weaker the N–O bond and the lower its ir stretching frequency. In contrast to CO, however, there is already an electron in the π^* orbital in neutral NO. This electron is readily transferred to the metal, nominally producing NO^+, and the transfer out of the antibonding π^* orbital accordingly strengthens the N–O bond and raises the ir stretching frequency.

Different transition metal ions may exhibit various modes of NO bonding depending on parameters such as their electronic structure and their coordination (*24*). NO may be bonded as linear or bent monomers, dimers, dinitrosyls, or polynitrosyls. In actual catalysts several nonequivalent transition metal ions may exist giving rise to quite complicated spectra. For example, Peri (*25*) found eight bands when NO was adsorbed on an alumina-supported chromia catalyst and assigned these to a mixture of monomers, dimers, and dinitrosyls. On the other hand NO has been reported to adsorb mainly as a mixture of monomers and dimers on silica-supported chromia catalyst (*26*) or mainly as dinitrosyls on Cr-X and Cr-Y zeolites (*27*). Furthermore, in certain cases, the NO may undergo reactions. Such reactions may in some catalysts take place even at room temperature. For example, Davydov and Bell (*28*) found that the initial adsorption of NO on a reduced Ru/SiO_2 catalyst occurs dissociatively and partially oxidizes the Ru. The subsequent NO adsorption was thus observed to take place predominantly on these oxidized species.

It is evident that the nature of the adsorption process and the interpretation of the absorption bands may be quite complex. Despite this, NO adsorption can still provide detailed information about the nature of the surface phase in Al_2O_3-supported Co, Mo, and Co–Mo catalysts, as is discussed below.

(A) Mo/Al_2O_3

The results on the Mo/Al_2O_3 catalyst (Fig. 1) show that the calcined state of the catalyst without pretreatment or only degassed at low temperature does not adsorb NO. It is generally believed (e.g., Ref. (*29*)) that in calcined Mo/Al_2O_3 catalysts the Mo is present as Mo^{6+}. Molybdenum in this state has a d^0 structure, and is thus not expected to adsorb NO strongly.

On the other hand, absorption bands were observed when the sample was evacuated at elevated temperatures (Figs. 1a and b). These results show that the pretreatments modify the surface as to create Mo in configurations capable of adsorbing NO. Such species are most likely to be some coordinatively unsaturated forms of Mo with valence states lower than 6 and they become more abundant with increasing evacuation temperature.

It is interesting that similar bands are observed for NO adsorbed on hydrogen-reduced Mo/Al_2O_3 catalysts (*9, 14, 16*), and thermally activated supported $Mo(CO)_6$ catalysts (*15*). In these studies it was concluded that the two NO bands are strongly coupled as in, for example, a dimeric or dinitrosyl species.

The present results also indicate that the two bands are related to the same adsorbed NO species. The fact that the adsorption complex is stable well above room temperature seems to favor a dinitrosyl species as opposed to a dimeric species. The observed frequencies are also typical of other molybdenum dinitrosyl species (Table 4). Thus, following this interpretation, the high-frequency band arises from the symmetric stretching mode, whereas the low-frequency band is due to the asymmetric stretching mode. The relative intensity of the two bands is related to the angle 2θ between the two N–O bond directions by the relation (*30*):

TABLE 4

Infrared Parameters for Some Cobalt and Molybdenum Dinitrosyl Adsorption Complexes

System	ν_{NO} (cm^{-1})	2θ (°)	$\bar{A} \times 10^{17}$ (cm/molecule)[a]	Ref.
	Cobalt systems			
$CoAl_2O_4$ (Type I)	1860,1780	115	1.3	This work
Co/Al_2O_3 (≤2% Co) (Type II)	1860–1870, 1780–1795	120–130	0.8–1.0	This work
Co_3O_4 (Type III)	1865, 1780	≲110	~0.3	This work
$Co–Mo/Al_2O_3$ (Type IV)	1880–1890, 1795–1805	112	2.1	This work
Co^{2+}-Y zeolite	1910, 1830	123		(*42*)
Co/SiO_2	1875, 1797	110		(*43*)
$[Co(NO)_2Cl]_2$	1859, 1790	110		(*44*)
$[Co(NO)_2I]_x$	1846, 1792	118		(*45*)
$[Co(NO)_2(NO_2)]_x$	1878, 1783	112		(*46*)
	Molybdenum systems			
Mo/Al_2O_3 calcined (Type V)	1804, 1692 1807[b], 1708[b]	103	2.5	This work
$Co–Mo/Al_2O_3$ calcined	~1800, 1695			This work
Mo/Al_2O_3 reduced	1804–1820, 1690–1710			(*9, 14, 16*)
$Mo(CO)_6/Al_2O_3$	1815, 1705			(*15*)
$[Mo(NO)_2Cl_2]_n$	1805, 1690			(*47*)
$Mo(NO)_2Cl_2[P(C_6H_5)_3]_2$	1790, 1670			(*48*)

[a] $\bar{A}$ is the integral molecular absorption coefficient defined by: $\bar{A} = (1/c \cdot l) \int \ln (I_0/I)\, d\nu$, where c is the concentration (molecules/g), l the thickness (g/cm²), I_0 the intensity of the incident radiation, and I the intensity of the emerging radiation.

[b] Obtained with a different alumina support.

$$I_{\text{symmetric}}/I_{\text{asymmetric}} = \cot^2 \theta. \quad (1)$$

For the $Mo(NO)_2$ species this intensity ratio is 0.63, which corresponds to $2\theta = 103°$.

Although the frequencies of the NO absorption bands are the same for the high-temperature evacuated and the hydrogen-reduced Mo/Al_2O_3 catalysts, the total band intensity is much lower for the evacuated catalysts (*16*). This indicates that only a small fraction of the Mo atoms at the surface of the alumina are reduced by the evacuation pretreatment to a state capable of adsorbing NO. In fact, the volumetric NO chemisorption results (Table 2) show that less than 1% of the Mo atoms are adsorbing NO.

Several investigators (*6, 31–37*) have shown that in catalysts with less than about 10% Mo, the molybdenum may exist as both tetrahedral monomeric species (Mo_T) and as polymeric species with molybdeum in octahedral coordination (Mo_O). Reduction studies of such catalysts have shown that Mo_T is resistant toward reduction, whereas Mo_O is reducible (*6, 34, 37*). It is thus possible that Mo reduced by the evacuation pretreatment is related to some form of polymeric Mo (or possibly trace amounts of MoO_3) which may easily achieve the

proper state of reduction and degree of coordinative unsaturation. Moreover, the very low NO band intensity observed for the Mo/Al_2O_3 catalyst prepared by impregnating aluminum hydroxide is in accord with the above since such a catalyst presumably contains more tetrahedrally coordinated molybdenum and aluminum molybdate-like configurations.

(B) Cobalt Model Compounds and Co/Al_2O_3 Catalysts

As for the Mo/Al_2O_3 catalysts, the Co/Al_2O_3 catalysts also show two bands after NO adsorption but the frequencies of the bands are different for the two catalyst systems.

Before discussing in detail the NO adsorption results on the Co/Al_2O_3 catalyst, the NO adsorption behavior on $CoAl_2O_4$ and Co_3O_4 will be considered since these compounds represent two extreme situations which might be encountered in calcined Co/Al_2O_3 catalysts. $CoAl_2O_4$ represents a case where all Co atoms have interacted with the support, whereas Co_3O_4 represents the situation where no interaction with the support occurs.

$CoAl_2O_4$

Yao and Shelef (*19*) attempted to study volumetrically the adsorption of NO on $CoAl_2O_4$ but observed no appreciable adsorption. Also, the Co ions were found by ion-scattering spectroscopy to be largely shielded from the surface (*38*). This was explained by a tendency (*39*) of tetrahedral cations in the spinel structure to move below the surface thus becoming more shielded than cations in octahedral sites. However, the present ir and volumetric chemisorption results (Table 3) show that some adsorption of NO on $CoAl_2O_4$ does take place and gives rise to two distinct ir absorption bands (Fig. 2). The NO adsorption may be related to the presence of octahedrally (or incipient-octahedrally) coordinated Co^{2+} ions since $CoAl_2O_4$ is not a completely normal spinel. The increase in adsorption which is observed (Fig. 2) for the $CoAl_2O_4$ sample after pretreatment at a higher temperature seems to confirm this proposal since it is known (*40, 41*) that the fraction of Co atoms located in octahedral coordination (or the degree of inversion of the spinel structure) increases by such a treatment. It can also be added that Yao and Shelef (*19*) did observe that compounds containing octahedrally coordinated Co readily adsorb NO.

Adsorption of NO on $CoAl_2O_4$ occurs apparently in two modes. One type of adsorption gives a species which is easily removed by room-temperature evacuation and produces a band at around 1875 cm^{-1}. This species most probably corresponds to a weakly bound mononitrosyl. After evacuation, bands at 1875 and 1790 cm^{-1} remain. The increase in the evacuation temperature affects the absolute but not the relative intensity of these bands. Thus, these bands belong to the same adsorpton complex, which is probably a dinitrosyl species. In fact, the frequencies, as well as the angle 2θ, agree rather well with those reported for other cobalt dinitrosyl species (Table 4). The value of 2θ suggests that the adsorption complex may have tetrahedral symmetry which is also found for the other Co dinitrosyl complexes (Table 4). The results that the octahedrally coordinated cobalt ions after NO adsorption become quasi-tetrahedrally coordinated show that the NO adsorption process extracts (or "reconstructs") the surface Co atoms.

Co_3O_4

The study of NO adsorption on Co_3O_4 is complicated by the fact that the high-temperature evacuation pretreatment causes drastic changes in the structure of the sample. This pretreatment not only removes species adsorbed at the surface but apparently leads to bulk reduction of the Co_3O_4 to CoO as shown by the X-ray diffraction results and thus the spectra correspond to adsorption on CoO. The importance of the pretreatment procedure is further discussed

elsewhere (*49*). The ease with which the changes occur may be related to both the structural similarity of CoO and Co_3O_4 (both having similar closed-packed oxygen lattices) and the multivalent character of the Co ion. Upon admission of NO to the pretreated Co_3O_4 sample, a broad band appears (Figs. 3a and b) which contains definite contributions around 1790, 1850, and 1870 cm^{-1}. The 1850-cm^{-1} band is very intense and the I_A/I_B ratio (Table 1) is by far the highest of all the samples studied. Most probably the 1850-cm^{-1} band is due to a weakly held mononitrosyl which can be removed by evacuation at room temperature (Fig. 3c). The large changes occurring as a result of evacuation at room temperature give rise to the smallest R value for all the cobalt samples (Table 1). As discussed in the following sections, this feature, as well as the high I_A/I_B ratio, can be used as fingerprints for the presence of Co_3O_4 in calcined Co and Co–Mo catalysts.

The two bands at 1790 and 1870 cm^{-1} that remain after evacuation at room temperature probably arise mainly from a dinitrosyl species. The high I_A/I_B intensity ratio corresponds to a relatively small angle (84°) between the two NO groups. This could indicate an octahedral adsorption complex but in view of the somewhat larger angles observed for all the other cobalt dinitrosyls (Table 4) it is also conceivable that the mononitrosyl species have not been completely removed by evacuation at room temperature.

In CoO, cobalt is octahedrally coordinated. Thus, similar to that for $CoAl_2O_4$, the adsorption of NO seems to involve octahedrally (or incipient-octahedrally) coordinated Co^{2+} cations. However, in the present case, the NO adsorption may also lead to reconstruction of the surface Co atoms.

Co/Al_2O_3 Catalysts

Most previous studies of calcined Co/Al_2O_3 catalysts have dealt with the bulk properties and have, therefore, given no direct information on the Co atoms possibly exposed at the surface of such catalysts. In order to obtain surface information, Ratnasamy and Knözinger (*7*) used ir studies of CO adsorption. No absorption bands were observed and the authors concluded that the Co atoms associated with the alumina are not exposed at the surface but are located in subsurface positions. However, the present results show that such catalysts do adsorb NO, and that Co must be located in surface positions. Therefore, the reported absence of CO adsorption seems to be linked to an inability of the surface Co to adsorb CO strongly rather than to the absence of surface cobalt atoms. Indeed, it has been reported for CoO–MgO catalysts (*50*) that NO adsorbs more strongly than CO. NO, therefore, appears to be a better probe molecule than CO for investigation of the surface cobalt atoms.

One interesting feature of the NO adsorption results on Co/Al_2O_3 catalysts is the ability to probe the changes occurring when the loading is varied. These changes indicate that the nature of the exposed Co atoms is different in low-loading ($\lesssim$2% Co) and high-loading ($\gtrsim$2% Co) catalysts.

Co/Al_2O_3 catalysts with $\lesssim$2% Co. The two low-loading catalysts (0.26% Co/Al_2O_3 and 2% Co/Al_2O_3) give rise to spectra (Figs. 4a and b) with quite similar spectral parameters (Table 1) during adsorption and desorption. The adsorption of NO on catalysts in this loading region was termed Type II. When the loading is increased from 0.26 to 2%, one observes a marked increase in the NO uptake (Fig. 6a) and the total absorbance (Fig. 6b) indicating that the main difference between catalysts in this region is in the amount of exposed Co atoms rather than in the nature of such atoms. The results given in Table 2 show that a large fraction of the total number of Co atoms in such catalysts are surface atoms.

It is seen from Table 1 that the Type II adsorption is quite different from the Type III adsorption which was observed for the Co_3O_4 sample, but it has many similarities

with the adsorption on $CoAl_2O_4$ (Type I). In spite of this similarity to the adsorption on $CoAl_2O_4$, there are small differences and therefore we do not propose that $CoAl_2O_4$ as such is present in these Co/Al_2O_3 catalysts. Rather, the Co is present in similar local surroundings but in more dilute concentrations than those Co atoms which adsorb NO in $CoAl_2O_4$. This is supported by the observation that the catalysts with the lowest surface concentration of active Co atoms exhibit band frequencies, as well as other spectral parameters, which differ most from those observed for $CoAl_2O_4$. The observation that the frequencies are higher for the "dilute" catalysts indicates that the Co atoms in these catalysts have less electrons available for back-donation to the adsorbed NO than in the more concentrated samples. Similar concentration-dependent frequency changes are observed for the calcined Co–Mo catalysts and for sulfided samples.

As was the case with $CoAl_2O_4$, the adsorption of NO on the low-loading catalysts can be characterized by the presence of two different forms of adsorbed NO, a mononitrosyl and a dinitrosyl. The angle 2θ between the two NO groups is calculated from the relative absorbances (I_A/I_B), using Eq. (1), to be around 120 to 130° for the different Co/Al_2O_3 catalysts indicating that the adsorption complex has a tetrahedral-like coordination. However, in view of the above discussion for $CoAl_2O_4$ and the results discussed below it seems likely that the Co atoms capable of adsorbing NO in the calcined catalyst were octahedrally coordinated prior to pretreatment and adsorption.

The above results suggest that at least part of the Co ions are present as octahedral ions at the surface of calcined Co/Al_2O_3 catalysts. This is interesting in view of the tendency of Co to occupy tetrahedral positions in alumina and in $CoAl_2O_4$. Several years ago Tomlinson *et al.* (*51*) suggested that octahedral Co ions may form due to the presence of octahedral vacancies in the alumina lattice, which has a defect spinel structure. The above authors proposed that during calcination of an impregnated and dried catalyst the Co ions, adsorbed at the alumina surface, may enter some of the octahedral vacancies. This mechanism for formation of octahedrally coordinated Co ions should be quite unique for catalysts made by impregnation and should not apply for catalysts made by coprecipitation. Indeed, Richardson and Vernon (*52*) found that coprecipitated Co/Al_2O_3 catalysts with low metal loading predominantly contained tetrahedral cobalt ions.

The present results lend further support to the mechanism proposed for the formation of octahedral Co ions since it is shown that such Co ions are indeed located at the surface. In fact, it seems that the fraction of Co atoms adsorbing NO corresponds rather closely to the fraction of Co atoms in octahedral positions. For example, Ashley and Mitchell (*11*) estimated from the magnetic measurements of Tomlinson *et al.* (*51*) that about 66% of the Co atoms in a 0.34% Co/Al_2O_3 catalyst were octahedral. Magnetic measurements (*53*) on the 0.26% Co/Al_2O_3 catalyst studied here indicate that the fraction of octahedral cations is slightly smaller for this sample. The 0.26% Co/Al_2O_3 catalyst adsorbs NO (Table 2) in an amount which corresponds to 1.05 mol NO/mol Co in the sample. Since the NO is adsorbed as a dinitrosyl, the adsorbed amount corresponds to about 53% of the Co atoms adsorbing NO, a value which is close to the estimated fraction of octahedrally coordinated Co ions. The tetrahedrally coordinated Co ions giving rise to the triplet in the uv spectra are most likely positioned in the subsurface regions of the alumina.

Upon increasing the calcination temperature, a decrease in the NO adsorption is seen (Fig. 7 and Table 2), but the type of NO adsorption remains the same (Table 1). At the same time, an increase in the amount of tetrahedral Co occurs, as noted, for example, by the change in color to deep blue. Thus, at higher calcination temperatures the Co ions diffuse from the octahedral po-

sitions at the surface to tetrahedral positions inside the Al_2O_3 lattice. Nevertheless, even after calcination at 923 K a significant fraction (~13% for the 2% Co/Al_2O_3 catalyst) of the Co cations is still located in octahedral positions at the surface. Recent Mössbauer results (*20*) are in agreement with this proposal.

Co/Al_2O_3 catalysts with ≳2% Co. When the cobalt loading is raised from 2 to 6.5%, the NO adsorption changes character (Figs. 4, 5 and Table 1) such that adsorption on the latter sample resembles that on the Co_3O_4 samples. X-Ray diffraction results confirm the presence of Co_3O_4 in the calcined 6.5% Co/Al_2O_3 catalysts. The presence of Co_3O_4 in high-loading Co/Al_2O_3 catalysts has also been observed by other investigators (e.g., Refs. (*11, 20, 37, 51, 52, 54*)). In the following we will discuss some possible explanations for the loading dependence of the nature and the amount of NO adsorbed. The observation of Co_3O_4 in catalysts with high loadings could be explained by the existence of only a limited number of sites on the alumina surface for binding Co atoms. These sites become progressively filled as the Co concentration increases and once all the surface sites are filled, excess Co will form Co_3O_4. According to the above picture, which is illustrated by Scheme 1 in Fig. 11, one would expect an almost linear increase in the amount of NO adsorbed with increasing cobalt loading until the surface sites have become saturated. Beyond this point the increase in the amount of adsorbed NO will depend on the degree of dispersion of the "excess" Co_3O_4. This situation, which corresponds to a curve lying in region 1 in Fig. 6a, is clearly not in accord with the marked decrease actually observed for high loadings in both the NO uptake and the absorbances. Thus, it appears that not only is Co_3O_4 formed in the high-loading catalysts but the number of Co atoms present at the surface of the alumina actually decreases below the number in the low-loading catalysts. In fact the concentration of Co at the surface of the alumina in such catalysts may be very low since the amount of NO chemisorbed on the 6.5% Co/Al_2O_3 catalyst may be explained by the cobalt being present entirely as Co_3O_4. A schematic model for all the Co/Al_2O_3 catalysts taking the above features into account is depicted in Scheme 2 in Fig. 11.

The phenomenon that, for high-loading Co/Al_2O_3 catalysts, Co_3O_4 may dominate at the expense of cobalt associated with the alumina is also consistent with magnetic (*51, 53*), Mössbauer (*20*), and gravimetric (*37*) results. A plausible explanation may be that during the preparation of the catalysts two parallel processes can occur, one leading to cobalt associated with the alumina and the other leading to formation of Co_3O_4. The former process dominates when the concentraton is low, whereas the latter seems to dominate for high-loading catalysts. An alternative explanation may be that during the calcination Co atoms migrate from the surface of the alumina to the Co_3O_4 phase. Clearly, further experiments are required to understand in more detail the processes involved in the genesis of such catalysts. This problem seems interesting in view of recent results (*21, 37*) which show that similar phenomena occur in $Co–Mo/Al_2O_3$ catalysts.

(C) $Co–Mo/Al_2O_3$ Catalysts

The literature on the location of the Co and Mo atoms in calcined $Co–Mo/Al_2O_3$ catalysts is at considerable variance (e.g., Refs. (*29, 55*)). For example, some investigators claim that the Co atoms are located entirely inside the alumina lattice while others claim that the cobalt may be present at the surface of the alumina as separate Co phases such as CoO or Co_3O_4. In view of the present results it is interesting to recall that several investigators have presented evidence for interactions between Co and Mo atoms. This interaction has been proposed to lead to formation of $CoMoO_4$ (usually for catalysts containing excess Mo), poorly crystallized cobalt molybdate-like species (*34, 56*), a Mo_4Co surface com-

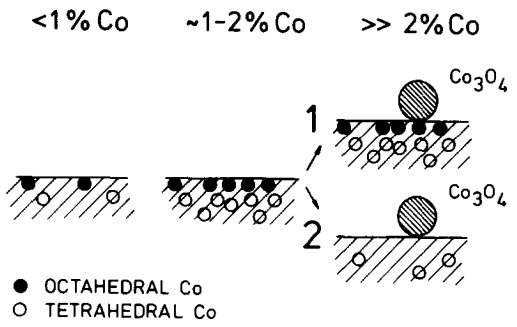

FIG. 11. Schematic models for the Co/Al_2O_3 catalysts. Scheme 1 represents the situation where cobalt enters the alumina until saturation is reached; excess cobalt is present as Co_3O_4. In Scheme 2 the formation of Co_3O_4 is accompanied by a decrease in the amount of cobalt associated with the alumina.

pound (*57*) Co–Mo bilayers (*8, 58–61*), and other often nonspecified forms (*2, 7, 12, 20, 21, 37, 62, 63*).

The present ir results on the $Co–Mo/Al_2O_3$ catalysts show that NO adsorbs on both Co and Mo atoms with the adsorption on the Co atoms being dominant. It is therefore clear that the Co atoms are not all situated inside the alumina lattice as suggested, for example, in the original monolayer model (*64*). The manner in which the two absorption bands disappear together upon evacuation suggests that the bands arise mainly from a dinitrosyl cobalt complex. This has recently been confirmed by a $^{15}NO–^{14}NO$ adsorption study (*49*).

The adsorption on the molybdenum atoms (Fig. 8a) is seen to be similar to that in the Mo/Al_2O_3 catalyst (Fig. 8c). However, it is apparent that the adsorption on the Co atoms in the $Co–Mo/Al_2O_3$ catalysts (Fig. 8a) is very different from that observed on the Co/Al_2O_3 catalyst with similar Co loading (Fig. 8b). This difference in adsorption indicates that a Co–Mo interaction phase has formed. This conclusion is further supported by the observation that the adsorption on the $Co–Mo/Al_2O_3$ catalyst is not only different from the adsorption on the Co/Al_2O_3 catalyst with the similar Co loading but is also very different from the adsorption on the Co/Al_2O_3 catalysts with both lower and higher Co loadings. In fact, the Type IV adsorption observed for the $Co–Mo/Al_2O_3$ catalyst differs from that of all the other Co systems studied (see Tables 1 and 4).

In order to elucidate the nature of the Co–Mo interaction phase in the $Co–Mo/Al_2O_3$ catalysts, a comparison with NO adsorption studies on $Co–Mo/SiO_2$ catalysts is helpful. For the latter catalysts it is observed (*49*) that the two absorption bands on both the Co and the Mo atoms are shifted with respect to those observed in Co/SiO_2 and Mo/SiO_2 samples, whereas as mentioned above the Mo bands are similar in the $Co–Mo/Al_2O_3$ and Mo/Al_2O_3 catalysts. This indicates that the interaction of the molybdenum with the support is much stronger (for catalyst with less than "monolayer" coverage) in the alumina-supported than in the silica-supported catalysts such that the molybdenum is present in similar surroundings, irrespective of cobalt being present or not. On the other hand, in the case of silica-supported catalysts, the interaction between Co and Mo is greater than the interaction of these elements with the silica support. Recent EXAFS measurements of alumina-supported catalysts (*63*) also show that the local structural surroundings of the Mo atoms are not greatly affected by the presence of Co atoms. The Co–Mo interaction phase for $Co–Mo/Al_2O_3$ catalysts is therefore not in the form of the $CoMoO_4$ or $CoMoO_4$-like phases observed for SiO_2-supported catalysts (*66*). Nevertheless, the interaction phase may have as discussed below some structural features in common with $CoMoO_4$.

In $CoMoO_4$, both the Mo and the Co atoms are octahedrally coordinated and the structure consists of groups of chains of edge-sharing CoO_6 and MoO_6 octahedra (*65*). In view of the results of NO adsorption on Co model compounds and catalysts, the cobalt atoms may be octahedral (before the adsorption of NO). In order that a structural description of the Co–Mo interaction phase can satisfy the criteria of having the

Co atoms in octahedral (or incipient-octahedral) coordination and of having the Mo atoms in a "monolayer" structure it seems reasonable that the Mo atoms involved in the Co–Mo interaction phase are those octahedrally coordinated and located in one-dimensional chains on the alumina surface (*7, 34*). The Co atoms are probably present as CoO_6 octahedra associated with these chains. In agreement with the above picture of the Co–Mo interaction phase Medema *et al.* (*34*) observed that Co–Mo/Al_2O_3 catalysts have a greater fraction of Mo atoms present in the polymeric (chain-like) form than Mo/Al_2O_3 catalysts. It could further be added that the large isomer shift and quadrupole splitting in the Mössbauer spectra of such catalysts (*20, 21*) are also in accordance with the Co atoms being octahedrally coordinated in the Co–Mo interaction phase.

The results on the Co–Mo/Al_2O_3 catalysts containing a very high Co loading (Fig. 10 and Table 1) indicate that Co_3O_4 has formed. This behavior is similar to that observed for the Co/Al_2O_3 catalysts. However, the Co concentration required to observe Co_3O_4 appears to be higher for the Co–Mo/Al_2O_3 catalysts than for the Co/Al_2O_3 catalysts. These findings are in agreement with other experiments on similar catalysts (*7, 20, 21, 37, 54*). The presence of the Co–Mo interaction phase may be the reason for this behavior, since the interaction may suppress the formation of the separate cobalt oxide phase.

Upon increasing the calcination temperature of the low-Co-loading catalyst from 773 to 923 K it is observed (Fig. 9) that the intensity of the absorption bands on cobalt decreases suggesting that some of the Co atoms have diffused into the alumina. The NO uptakes have also decreased accordingly (Table 2). Besides a frequency shift which is quite similar to those observed for Co/Al_2O_3 catalysts (Fig. 7), the ir parameters (Table 1) of the high- and low-temperature calcined Co–Mo/Al_2O_3 catalysts are very similar indicating that the major changes are in the number of Co atoms located in the Co–Mo interaction surface phase rather than in its characteristics. In view of previous studies of the effects of high-temperature calcination (*8*), it is interesting that the present results have shown that the Co–Mo interaction phase is not destroyed by such a treatment and that a significant number of promoter atoms still remain at the surface in this phase.

V. CONCLUSIONS

From the data presented above it is concluded that NO adsorption studies are useful in characterizing the calcined precursors for Co–Mo/Al_2O_3 HDS catalysts. From the ir spectra one can distinguish between cobalt and molybdenum atoms located at the surface of the catalysts and changes in the nature of the phases in which these atoms are situated may also be revealed. Consequently, it may be possible to obtain information regarding the relative importance of different phases in forming the active species in the sulfided catalysts. In this connection the presence of the Co–Mo surface phase seems particularly interesting since it may be a likely precursor to the active Co–Mo–S phase (*66, 67*), the formation of which has been shown (*66, 68*) to be favored by an intimate contact between the Co and Mo atoms before the sulfiding. This possibility is presently being investigated.

ACKNOWLEDGMENTS

The authors wish to thank B. S. Clausen and R. Candia for many stimulating discussions throughout this work. Fruitful discussions with J. A. Dumesic, F. E. Massoth, and R. F. Howe are also acknowledged and J. W. Hightower is thanked for bringing our attention to the work of J. R. Hardee, Jr., prior to its publication. Finally, the authors are grateful to J. Villadsen for providing X-ray analysis results and to K. Reiter and S. V. Christensen for technical assistance in carrying out infrared and chemisorption measurements.

REFERENCES

1. Lipsch, J. M. J. G., and Schuit, G. C. A., *J. Catal.* **15,** 174 (1969).

2. Mitchell, P. C. H., and Trifirò, F., *J. Catal.* **33,** 350 (1974).
3. Slager, T. L., and Amberg, C. H., *Canad. J. Chem.* **50,** 3416 (1972).
4. Kiviat, F. E., and Petrakis, L., *J. Phys. Chem.* **77,** 1232 (1973).
5. Giordano, N., Bart, J. C. J., Castellan, A., and Vaghi, A., *J. Less Common Met.* **36,** 367 (1974).
6. Ratnasamy, P., Ramaswamy, A. V., Banerjee, K., Sharma, D. K., and Ray, N., *J. Catal.* **38,** 19 (1975).
7. Ratnasamy, P., and Knözinger, H., *J. Catal.* **54,** 155 (1978).
8. Moné, R., *in* "Preparation of Catalysts" (B. Delmon, P. A. Jacobs, and G. Poncelet, Eds.), p. 381. Elsevier, Amsterdam (1976): Moné, R., and Moscou, L., *Amer. Chem. Soc. Symp. Ser.* **20,** 150 (1975).
9. Peri, J. B., *Amer. Chem. Soc. Div. Pet. Chem. Prepr.* **23,** 1281 (1978).
10. Hardee, J. R., Jr., Ph.D. dissertation, Rice University, 1978.
11. Ashley, J. H., and Mitchell, P. C. H., *J. Chem. Soc. A,* 2821 (1968).
12. Topsøe, N., *J. Catal.* **64,** 235 (1980).
13. Little, L. H., "Infrared Spectra of Adsorbed Species." Academic Press, New York, 1966.
14. Hall, W. K., and Millman, W. S., *J. Phys. Chem.* **83,** 427 (1979).
15. Kazusaka, A., and Howe, R. F., *J. Catal.* **63,** 447 (1980).
16. Topsøe, N., and Topsøe, H., to be submitted for publication.
17. Topsøe, H., Clausen, B. S., Burriesci, N., Candia, R., and Mørup, S., *in* "Preparation of Catalysts II" (B. Delmon, P. Grange, P. A. Jacobs, and G. Poncelet, Eds.), p. 479. Elsevier, Amsterdam, 1979.
18. Turnham, B., Ph.D. dissertation, Stanford University, 1975.
19. Yao, H. C., and Shelef, M., *in* "The Catalytic Chemistry of Nitrogen Oxides" (R. L. Klimisch and J. G. Larson, Eds.), p. 45. Plenum, New York, 1975.
20. Clausen, B. S., Ph.D. dissertation, Technical University of Denmark, 1979.
21. Wivel, C., Clausen, B. S., Candia, R., Mørup, S., and Topsøe, H., submitted for publication.
22. Terenin, A., and Roev, L., *in* "Actes 2me. Congr. Int. Catal., Paris, 1960," p. 2183. Editions Technip, Paris, 1961.
23. Shelef, M., and Kummer, J. T., *Chem. Eng. Prog. Symp. Ser.* **67,** 74 (1971).
24. Enemark, J. H., and Feltham, R. D., *Coord. Chem. Rev.* **13,** 339 (1974).
25. Peri, J. B., *J. Phys. Chem.* **78,** 588 (1974).
26. Kugler, E. L., Kadet, A. B., and Gryder, J. W., *J. Catal.* **41,** 72 (1976).
27. Pearce, J. R., Sherwood, D. E., Hall, M. B., and Lunsford, J. H., *J. Phys. Chem.* **84,** 3215 (1980).
28. Davydov, A. A., and Bell, A. T., *J. Catal.* **49,** 332 (1977).
29. Massoth, F. E., *in* "Advances in Catalysis and Related Subjects" (D. D. Eley, H. Pines, and P. B. Weiz, Eds.), Vol. 27, p. 265. Academic Press, New York, 1978.
30. Cotton, F. A., and Wilkinson, G., "Advanced Inorganic Chemistry," 3rd ed., p. 697. Interscience, New York, 1972.
31. Giordano, N., Bart, J. C. J., Vaghi, A., Castellan, A., and Martinotti, G., *J. Catal.* **36,** 81 (1975).
32. Brown, F. R., Makovsky, L. E., and Rhee, K. H., *J. Catal.* **50,** 162 (1977).
33. Brown, F. R., Makovsky, L. E., and Rhee, K. H., *Appl. Spectrosc.* **31,** 563 (1977).
34. Medema, J., van Stam, C., de Beer, V. H. J., Konings, A. J. A., and Koningsberger, D. C., *J. Catal.* **53,** 386 (1978).
35. Okamoto, U., Tomioka, H., Katoh, Y., Imanaka, T., Teranishi, S., *J. Phys. Chem.* **84,** 1833 (1980).
36. Knözinger, H., and Jeziorowski. H., *J. Phys. Chem.* **82,** 2002 (1978).
37. Chung, K. S., and Massoth, F. E., *J. Catal.* **64,** 320 (1980).
38. Shelef, M., Wheeler, M. A. Z., and Yao, H. C., *Surf. Sci.* **47,** 697 (1975).
39. Cimino, A., and Schiavello, M., *J. Catal.* **20,** 202 (1970).
40. Angeletti, C., Pepe, F., and Porta, P., *J. Chem. Soc. Faraday Trans. 1* **73,** 1972 (1977).
41. Porta, P., and Anichini, A., *J. Chem. Soc. Faraday Trans. 1* **76,** 2448 (1980).
42. Windhorst, K. A., and Lunsford, J. H., *J. Amer. Chem. Soc.* **97,** 1407 (1975).
43. Rebenstorf, B., *Acta Chem. Scand. Ser. A* **31,** 208 (1977).
44. Johnson, B. F. G., and McCleverty, J. A., *Prog. Inorg. Chem.* **7,** 277 (1966).
45. Dahl, L. F., deGil, E. R., and Feltham, R. D., *J. Amer. Chem. Soc.* **91,** 1653 (1969).
46. Strouse, C. F., and Swanson, B. I., *Chem. Commun.*, 55 (1971).
47. Johnson, B. F. G., *J. Chem. Soc. A,* 475 (1967).
48. Cotton, F. A., and Johnson, B. F. G., *Inorg. Chem.* **3,** 1609 (1964).
49. Topsøe, N., and Topsøe, H., *Bull. Soc. Chim. Belg.* **90**(12) 1311 (1981).
50. Hagan, A. P., Lofthouse, M. G., Stone, F. S., and Trevethan, M. A., *in* "Preparation of Catalysts II" (B. Delmon, P. Grange, P. A. Jacobs, and G. Poncelet, Eds.), p. 417. Elsevier, Amsterdam, 1979.
51. Tomlinson, J. R., Keeling, R. O., Rymer, G. T., and Bridges, J. M., *in* "Actes 2me. Congr. Int.

Catal. Paris, 1960," p. 1831. Editions Technip, Paris, 1961.
52. Richardson, J. T., and Vernon, L. W., *J. Phys. Chem.* **62,** 1153 (1958).
53. Clausen, B. S., Nevald, R., Candia, R., and Topsøe, H., unpublished results.
54. Lo Jacono, M., Cimino, A., and Schuit, G. C. A., *Gazz. Chim. Ital.* **103,** 1281 (1973).
55. Grange, P., *Catal. Rev. Sci. Eng.* **21**(1), 135 (1980).
56. Cheng, C. P., and Schrader, G. L., *J. Catal.* **60,** 276 (1979).
57. Grimblot, J., and Bonnelle, J. P., *J. Electron Spectrosc. Relat. Phenom.* 9, 449 (1976).
58. Apecetche, M. A., and Delmon, B., *React. Kinet. Catal. Lett.* **12,** 385 (1979).
59. Gajardo, P., Grange, P., and Delmon, B., *J. Catal.* **63,** 201 (1980).
60. Okamoto, Y., Imanaka, T., and Terinishi, S., *J. Catal.* **65,** 448 (1980).
61. Delannay, F., Haeassler, E. N., and Delmon, B., *J. Catal.* **46,** 469 (1980).
62. Richardson, J. T., *Ind. Eng. Chem. Fundam.* **3,** 154 (1964).
63. Clausen, B. S., Topsøe, H., Candia, R., Villadsen, J., Lengeler, B., Als-Nielsen, J., and Christensen, F., *J. Phys. Chem.* **85,** 3868 (1981).
64. Schuit, G. C. A., and Gates, B. C., *AIChE J.* **19,** 417 (1973).
65. Smith, G. W., and Ibers, J. A., *Acta Crystallogr.* **19,** 269 (1965).
66. Topsøe, H., Clausen, B. S., Candia, R., Wivel, C., and Mørup, S., *Bull. Soc. Chim. Belg.* **90**(12) 1189 (1981).
67. Wivel, C., Candia, R., Clausen, B. S., Mørup, S., and Topsøe, H., *J. Catal.* **68,** 453 (1981).
68. Topsøe, H., Clausen, B. S., Candia, R., Wivel, C., and Mørup, S., *J. Catal.* **68,** 433 (1981).